Automatic detection and correction of aerodynamic and inertial rotor imbalances in wind turbine rotors

M. Bertelè, C.L. Bottasso

Wind Energy Institute, Technische Universität München, Garching bei München, Germany

E-mail: marta.bertele@tum.de

Abstract. In this work, a novel rotor rebalancing algorithm is tested in a simulation environment to evaluate its performance when facing both aerodynamic and inertial imbalances. The algorithm, starting from a generic measurement collected on the wind turbine fixed frame, is capable of remotely minimizing once per revolution vibrations, avoiding the need for on-site inspections, and without requiring detailed information about the machine. Indeed, once access to the pitch system is granted, this algorithm simply iteratively computes the pitch angle that needs to be applied to each individual blade in order to rebalance the rotor.
Several turbulent time histories, with changing mean inflows, were simulated with the goal of testing the proposed method in realistic field conditions. Overall, the algorithm proved capable of significantly reducing the desired once per revolution vibrations in 3 to 4 iterations, irrespective of the imbalance root cause, its severity and its location. The method also appeared quite robust, showing that the found rebalanced configurations guarantee reduced vibrations no matter the machine operating point.

1. Introduction

Operation and maintenance (O&M) costs constitute a significant driver for the overall cost of energy. This is particularly true especially for offshore installations, where on-site inspections can make up for about 30% of the overall costs [2]. Of all major systems, the power and rotor modules account for about 50% of the failure rate, and specifically the pitch system is one of the most delicate, being responsible for 15% of the overall yearly faults [14]. Moreover, a fault in the pitch system can be quite critical because it results in a significant downtime (about 20% of the overall downtime), since on site visual inspections are usually necessary to detect a fault in a pitch sensor, in a pitch actuator or an offset due to incorrect blade installation.
Such faults in the pitch system not only might affect power production, but might also have a significant impact on the integrity and fatigue life of major components. Indeed, when a pitch offset is present among the blades, irrespective of its root cause, the rotor becomes aerodynamically imbalanced, leading in turn to additional loading and vibrations in the fixed frame. Certification guidelines instruct to verify the effects of pitch offsets as large as ± 0.3 deg, showing how relatively small misalignments need to be taken into consideration (GL Standards, 2010, Sect. 4.3.4.1, pp. 4–20). Unfortunately, small misalignments are quite common: a recent analysis comprising about 192 turbines [13] shows that about 62% of the considered machines suffered from a pitch misalignment up to 0.6 deg, 25% between 0.6 and 1 deg, and 13% between 1 to 2 deg.


Content from this work may be used under the terms of the Creative Commons Attribution 3.0 licence. Any further distribution of this work must maintain attribution to the author(s) and the title of the work, journal citation and DOI.
Published under licence by IOP Publishing Ltd

The second major cause for imbalanced rotors are inertial imbalances. Indeed, mass imbalances can be quite common, since one just needs to install blades of slightly different weight to generate an inertial imbalance. Also in this case, detecting and correcting such issues can be quite costly, since one needs to be on site to apply trial and correction masses on the turbine rotor. Of course, often rotors can suffer from a combination of aerodynamic and inertial imbalances, making the detection and correction process even more complex.

Nowadays, the detection of rotor imbalances usually relies on the analysis of the vibrations in the machine fixed frame. For example, Niebsch et al. [10] and Niebsch and Ramlau [9] proposed a method to simultaneously estimate both mass and aerodynamic imbalance effects from nacelle vibrational measurements. Nevertheless, this methodology requires a finite element model of the machine, therefore significantly hindering its applicability. A different approach was proposed by Kusnick et al. [8], where the blade misalignment estimation is performed by an ad hoc workflow using multiple measurements, including power output, blade loads and accelerations. Completely alternative approaches rely on the continuous action of the turbine controller to mitigate the effects of a rotor imbalance, rather than correcting for it, which might negatively affect the pitch system duty cycle [7, 4].

A different approach was presented by Bertelé et al. [1], which proposed an algorithm aiming at remotely correcting rotor imbalances by purposefully changing the pitch angles of the individual blades. In contrast to [7, 4], this algorithm does not require a continuous dynamic pitch action, bur rather on point steady corrections which are applied until the rebalancing is complete. Although this approach proved quite effective and robust, only aerodynamic imbalances were considered in the simulation study, leaving as open question if the proposed algorithm could be successfully employed also in the presence of an inertial imbalance.

Therefore, in this work the rebalancing methodology presented by Bertelé et al. [1] will be further tested to evaluate its performance in the presence not only of an aerodynamic imbalance but also of an inertial imbalance, and combinations thereof. The proposed algorithm, starting from a once per revolution (1P) signal measured in the turbine fixed frame, iteratively computes the required pitch offsets to be applied to each individual blade in order to minimize said 1P. This methodology could therefore be quite appealing, since it would allow for a remote rebalancing of the rotor irrespective of the imbalance root cause, without the need for shutdowns, costly on site inspections or detailed information about the machine.

The paper is organized as follows. Section 2 provides a brief overview of the rotor spectral analysis and a thorough description of the rebalancing algorithm. The algorithm performance is then tested in § 3, whereas § 4 concludes the paper presenting outlooks for future work.

2. Methodology

2.1. Rotor spectral analysis

It is common knowledge that a balanced wind turbine rotor acts as a filter, allowing loads to be transmitted from the rotating to the fixed frame only at frequencies multiples of the number of blades B. As an example, let's consider the nodding moment N, measured at the hub in the fixed frame. Such moment can be derived as follows

$$N = \sum_{i=1}^{B} m_i \cos \psi_i, \tag{1}$$

with i indicating the i$-th$ blade, ψ the azimuthal position, and m the blade out of plane moment, which can be in turn expanded in the following Fourier series

$$m_i = m_{0_i} + \sum_{n=1}^{\inf}(m_{\mathrm{nc}_i}\cos(n\psi_i) + m_{\mathrm{ns}_i}\sin(n\psi_i)), \tag{2}$$

where subscripts $()_{\mathrm{nc}}$ and $()_{\mathrm{ns}}$ represent the n-cosine and sine harmonic components.

Assuming a balanced rotor, i.e. all blades provide an identical but shifted in time contribution, it is easy to prove that the nodding moment at the hub is the sum of harmonics which are multiple of the number of blades. On the other hand, if the rotor were unbalanced, additional frequencies would be transmitted to the fixed frame, with the 1P usually the highest in amplitude. Therefore, in this work 1P signals are chosen as input parameter for the rebalancing algorithm of § 2.2. Generally, one can distinguish between two main sources of rotor imbalance: aerodynamic imbalance and mass imbalance. A brief overview is presented in the following.

Aerodynamic imbalance

The out of plane moment acting on the generic blade can be expressed as

$$m_i = \frac{1}{2}\rho ARV^2 C_m, \tag{3}$$

with ρ the air density, A and R the rotor area and radius, V the wind speed and C_m defined as $C_m(\beta, \lambda, q, \psi_i) = \frac{m_i}{0.5\rho ARV^2}$. This coefficient represents the adimensionalization of the out of plane moment, and therefore depends on the pitch angle β, the tip speed ratio λ ($\lambda = \Omega R/V$, with Ω the rotor speed), the dynamic pressure q and the blade azimuth angle ψ.

Let's now assume that the rotor is aerodynamically imbalanced. This might happen because of a fault in the pitch system (faulty sensor, faulty actuator) or simply because of a pitch offset generated during installation. If for simplicity we assume only blade one to be suffering from a pitch offset $\Delta\beta$, then one can rewrite the out of plane moment of the given blade as $m_1 = \frac{1}{2}\rho ARV^2\left(C_m + C_{m_\beta}\Delta\beta\right)$, with C_{m_β} the partial derivative of the moment coefficient with respect to the pitch angle. Starting from Eq. (1), it is easy to prove that $\Delta\beta$ will generate an additional 1P contribution to the nodding moment: this contribution depends on the dynamic pressure q, i.e. on the ambient conditions, and, in the proposed example, can be expressed as

$$N_{\mathrm{A}} = \frac{1}{2}\rho ARV^2 C_{m_\beta}\Delta\beta\cos\psi. \tag{4}$$

Mass imbalance

When a rotor is inertially imbalanced, for example because it's equipped with blades of different weight, additional 1P harmonics are transmitted to the fixed frame. In this case, the rotor eccentricity can be modelled by an additional mass M, located at a given radial distance r from the rotor centre and at a longitudinal distance l from the rotor plane. This mass is also placed at an azimuthal angle ψ_m from the azimuthal reference, Fig. 1.

Of course, whilst rotating M will be subjected to two contributions: the gravitational force Mg, with g the gravitational acceleration, and the centrifugal force

$$F_c = Mr\Omega^2. \tag{5}$$

Therefore, the contribution of such eccentricity to the nodding moment, neglecting any dynamics induced by rotor-nacelle couplings, can be computed as follows

$$N_{\mathrm{M}} = Mr(l\Omega^2 + g\sin(\zeta))\cos(\psi + \psi_m), \tag{6}$$

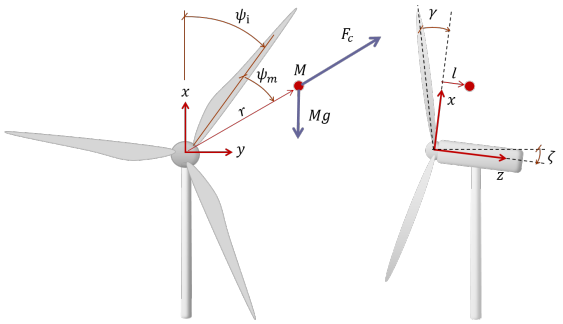

Figure 1. Modelling of a rotor eccentricity due to the presence of a mass imbalance.

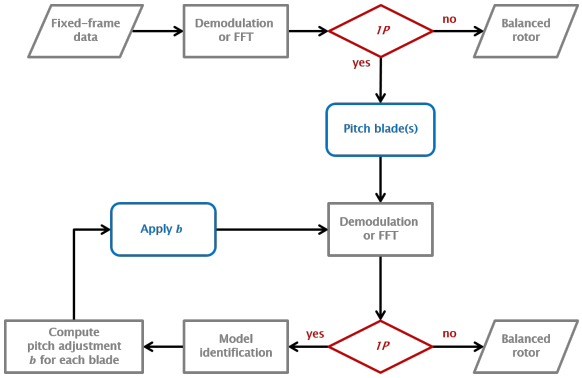

Figure 2. Graphical representation of the rotor rebalancing algorithm.

with ζ and γ the nacelle uptilt and the cone angle respectively. Interestingly, Eq. (6) shows that an inertial imbalance will generate 1P which is solely a function of Ω^2, making this contribution dependent on the turbine operating point.

2.2. Imbalance-disturbance model

In this work, any 1P harmonic measured in the fixed frame is related to pitch disturbances via the following linear model, already defined in [1]

$$\boldsymbol{s} = \boldsymbol{C}(\boldsymbol{b} - \boldsymbol{b}_m) = \boldsymbol{C}\boldsymbol{b} + \boldsymbol{s}_m, \tag{7}$$

where vector $\boldsymbol{b} = (b_1, b_2, b_3)^T$ contains the pitch adjustments b_i for each blade, $\boldsymbol{b}_m$ is the unknown pitch misalignment, and matrix $\boldsymbol{C}$ and vector $\boldsymbol{s}_m$ are the unknown model coefficients, where $\boldsymbol{C}$ can be defined as $\boldsymbol{C} = [c_{\mathrm{c}_1},\ c_{\mathrm{c}_2},\ c_{\mathrm{c}_3};\ c_{\mathrm{s}_1},\ c_{\mathrm{s}_2},\ c_{\mathrm{s}_3}]$. Finally, the 1P cosine and sine harmonic amplitude of a given fixed frame measurement are first scaled by the dynamic pressure and then collected in $\boldsymbol{s}$ as $\boldsymbol{s} = (s_{\mathrm{c}}, s_{\mathrm{s}})^T$. In a nutshell, the described model states that if one were to know the misalignment $\boldsymbol{b}_m$, by pitching the blades by $\boldsymbol{b} = \boldsymbol{b}_m$, one would rebalance the rotor, causing $\boldsymbol{s} = 0$. On the other hand, before rebalancing $\boldsymbol{b} = 0$, and therefore one could measure a 1P in the fixed frame equal to $\boldsymbol{s}_m = -\boldsymbol{C}\boldsymbol{b}_m$.

The decision to scale the 1P signals by q allows to take into account possible changes in ambient conditions and operating point during the identification or rebalancing phase. This clearly holds for the aerodynamic imbalances of Eq. (4), which are a function of q, but partially also for the inertial imbalances of Eq. (6), which are a sole function of Ω. Indeed, wind and rotor speed are proportional to the tip speed ratio $\lambda = \frac{\Omega R}{V}$, which is kept constant in region II. Therefore, since mass imbalances depend on Ω, by scaling by q within this region we can still expect to find a rebalanced configuration valid for multiple operating points, as long as no severe changes in density occur. On the other hand, outside region II, where λ is not constant, we can expect a performance degradation due to a non-exact rescaling.

To simplify the model identification, the number of unknown coefficients can be reduced by exploiting the radial symmetry of the rotor. Indeed, assuming a periodic response, the effects caused by a misalignment in the first blade will be the same as the effects of an equivalent misalignment in the second blade, only with a $2\pi/3$ phase shift. Therefore, the model coefficients are not independent:

$$\begin{Bmatrix} c_{\mathrm{c}_2} \\ c_{\mathrm{s}_2} \end{Bmatrix} = \begin{bmatrix} \cos(2\pi/3) & \sin(2\pi/3) \\ -\sin(2\pi/3) & \cos(2\pi/3) \end{bmatrix} \begin{Bmatrix} c_{\mathrm{c}_1} \\ c_{\mathrm{s}_1} \end{Bmatrix} = \boldsymbol{R}\boldsymbol{c}. \tag{8}$$

Clearly, the same argument holds for the relationship between the response of blades two and three. Therefore, matrix $\boldsymbol{C}$ only depends on the two coefficients of vector $\boldsymbol{c}$, and can be written as $\boldsymbol{C} = \left[\begin{array}{ccc} \boldsymbol{c} & \boldsymbol{Rc} & \boldsymbol{R^2c} \end{array} \right]$.

2.3. Model identification

To use the model to correct for a rotor imbalance, one needs to identify the unknown coefficients in Eq. (7). To this end, it is convenient to rewrite the imbalance-disturbance model as follows

$$\boldsymbol{s} = \boldsymbol{Cb} + \boldsymbol{s}_m = \boldsymbol{Bc} + \boldsymbol{s}_m. \tag{9}$$

where matrix $\boldsymbol{B}$ is a sole function of the pitch adjustment $\boldsymbol{b}$, and writes $\boldsymbol{B} = [B_{11},\ B_{12}; -B_{12},\ B_{11}]$, with $B_{11} = b_1 + \cos(2\pi/3)b_2 + (\cos(2\pi/3)^2 - \sin(2\pi/3)^2)b_3$, $B_{12} = \sin(2\pi/3)b_2 + 2\sin(2\pi/3)\cos(2\pi/3)b_3$.

Given the linearity of the model, one just needs to collect two measurement points to identify the unknown coefficients. The first measurement point can be sampled before starting the rebalancing procedure. In this condition, $\boldsymbol{b} = \boldsymbol{b}^{(0)} = 0$ and a 1P harmonic equal to $\boldsymbol{s}^{(0)}$ is measured on the machine. The second sample point can be collected after pitching the blades by a chosen arbitrarily amount $\boldsymbol{b}^{(1)}$, measuring a 1P harmonic equal to $\boldsymbol{s}^{(1)}$. Considering these two measurements together, one can write

$$\left\{ \begin{array}{c} \boldsymbol{s}^{(0)} \\ \boldsymbol{s}^{(1)} \end{array} \right\} = \left[\begin{array}{cc} \boldsymbol{B}^{(0)} & \boldsymbol{I} \\ \boldsymbol{B}^{(1)} & \boldsymbol{I} \end{array} \right] \left\{ \begin{array}{c} \boldsymbol{c} \\ \boldsymbol{s}_m \end{array} \right\}, \tag{10}$$

where $\boldsymbol{B}^{(0)}$ and $\boldsymbol{B}^{(1)}$ indicate matrix $\boldsymbol{B}$ evaluated in correspondence of vectors $\boldsymbol{b}^{(0)}$ and $\boldsymbol{b}^{(1)}$, respectively. Inverting this relationship, one obtains the unknown model coefficients $\boldsymbol{c}$ and $\boldsymbol{s}_m$.

2.4. Rebalancing

Once that model (7) has been identified, it can be used to rebalance the rotor. Still, one has to keep in mind that only imbalances among the blades will cause a 1P in the fixed frame. Indeed, any collective rotation of all blades will not generate an imbalance. As a consequence, to rebalance the rotor, i.e. to affect the 1P in the fixed frame, one needs to compute a pitch adjustment vector $\boldsymbol{b}$ such that $\sum_{i=1}^{3} b_i = 0$. Therefore, this "zero-collective" constraint is appended to model (7) leading to the following formulation

$$\left\{ \begin{array}{c} \boldsymbol{s} \\ 0 \end{array} \right\} = \left[\begin{array}{c} \boldsymbol{C} \\ \boldsymbol{1}^T \end{array} \right] \boldsymbol{b} + \left\{ \begin{array}{c} \boldsymbol{s}_m \\ 0 \end{array} \right\}, \tag{11}$$

where $\boldsymbol{1} = (1, 1, 1)^T$. Setting $\boldsymbol{s} = 0$, i.e. requesting a null 1P harmonic response in the fixed frame, one readily computes the necessary pitch adjustments as

$$\boldsymbol{b} = -\left[\begin{array}{c} \boldsymbol{C} \\ \boldsymbol{1}^T \end{array} \right]^{-1} \left\{ \begin{array}{c} \boldsymbol{s}_m \\ 0 \end{array} \right\}. \tag{12}$$

If after the re-adjustment a significant 1P is still detected, the method can be applied iteratively. The amplitude measured in the current configuration becomes the new data point that, together with the one measured before re-adjusting, can be used to re-identify the model. With the new model coefficients, Eq. (12) can be used to estimate a new pitch adjustment.
This iterative procedure can be repeated until a desired 1P threshold is achieved, and can compensate for possible non accounted non-linearities or severe changes in wind conditions and especially density, whose variations can negatively affect the rescaling of inertial-induced imbalances, §2.2. A graphical depiction of the rebalancing algorithm is presented in Fig. 2.

3. Results

3.1. Simulation environment

In this work, the behaviour of a 3MW horizontal axis wind turbine has been simulated. The machine has cut-in, rated and cut-off speed at 3, 12.5 and 25 m/s, and a hub height and a rotor diameter of 80 m and 93 m, respectively. The finite element multibody code `Cp-Lambda` [3] was used to simulate its dynamic behaviour, using geometrical exact non linear beam models and including rotor speed-dependent mechanical losses. The classical blade element momentum theory (BEM) is used to represent the aerodynamics, considering even hub and tip-losses, dynamic stall and unsteady effects. A speed-scheduled linear quadratic regulator (LQR) [12] models an active pitch/torque controller, while a first and second order system respectively are used to model torque and pitch actuators. The pitch actuator resolution is assumed to be 0.1 deg. Finally, in order to simulate realistic field conditions, several 10-minute long turbulent simulations were created using `TurbSim` [6], considering different wind speeds, densities, yaw misalignment angles and vertical shears.

In all simulations, both an aerodynamic and a mass imbalance were introduced in the model. The aerodynamic imbalance was modelled in the form of pitch offsets ranging from -2 to 2 deg applied to one or more blades. To quantify the severity of such aerodynamic imbalance, the absolute residual pitch misalignment angle ϵ left on the rotor was introduced and defined as

$$\epsilon = \max(\boldsymbol{b}_m - \boldsymbol{b}) - \min(\boldsymbol{b}_m - \boldsymbol{b}). \tag{13}$$

The inertial imbalance, on the other hand, was modelled by adding mass to one or more blades. The severity of the imbalance was quantified according to the G grade [5], which is defined as

$$G = \frac{U_{per} N}{9549 W} 10^6 R_{eff}, \tag{14}$$

with U_{per} the added mass, N the maximum rpm, W the rotor weight and R_{eff} the mass radial distance. Different G grades were chosen to try to represent realistic conditions, based on the data colleceted in [11], which reports the mass imbalances estimated on four Vestas V80-2MW machines.

3.2. Algorithm performance

The algorithm described in § 2.4 and already introduced in [1] is now tested in the presence of both aerodynamic and inertial imbalances. For the sake of clarity, in the following the initial imbalanced configuration will be referred to as $\mathrm{s}^{(0)}$, and the respective rebalanced configuration as $\mathrm{s}^{(\mathrm{R})}$.

Two different initial aerodynamic imbalances were considered: $\epsilon^{(0)} = [3.5,\ 0.5]$ deg. For each aerodynamic imbalance, also three different G grades were introduced, $G = [33,\ 83,\ 116]$, which correspond to a blade respectively $[3,\ 5,\ 7]\%$ heavier than nominal design. The algorithm was then applied iteratively with the aim of minimizing the 1P of the fore-aft acceleration at the nacelle main bearing. This acceleration signal was chosen as main driver simply because accelerometers tend to be more readily available on standard machines than strain gauges, given that they are easier to install. The 1P measurements were collected for 10 minutes, then averaged and fed to the algorithm. In addition, to replicate more realistic field conditions, the mean inflow was varied among the simulations, i.e. among the algorithm steps, as listed in Table 1.

Figure 3 (left) shows, for the larger initial aerodynamic imbalance $\epsilon^{(0)} = 3.5$ deg, the algorithm performance over the number of iterations. Looking at Fig. 3 (a), it is clearly

noticeable how the algorithm can successfully minimize the 1P fore-aft accelerations after 3 iterations for inertial imbalances G33 and G83, reaching its target of an almost 100% 1P reduction with respect to the initial configuration. One extra iteration is required for G116. This 1P reduction is of course achieved by reducing the residual pitch misalignment on the rotor, Fig. 3 (d). Moreover, the iterative nature of the algorithm proves capable of compensating also for changes in ambient density, which varies of about 10% within the rebalancing procedure (simulation 1 to 3).
Although in this work the algorithm only aims at reducing the fore-aft 1P acceleration, one could be interested in reducing additional 1P loadings, such as the nodding and yawing moments measured at the hub. Therefore, Fig. 3 (b) and (c) report the variations in these quantities respectively. Also in this case, the algorithm can successfully reduce nodding and yawing 1P of almost 100% with respect to the initial configuration.

Similar results were obtained starting from an initial aerodynamic imbalance of $\epsilon^{(0)} = 0.5$ deg, Fig. 3 (right). While the algorithm needs two iterations to rebalance the rotor for G33, three iterations are required for larger inertial imbalances. As in the previous examples, the fore-aft 1P accelerations are successfully minimized thanks to the decreased ϵ, and a decrease in nodding and yawing moments is also noticeable. Still, in the G116 case, the moment reduction appears relatively small. When looking at these results, one should nevertheless remember that, in this work, the goal of the algorithm is merely to reduce the 1P fore-aft accelerations: to reduce other relevant quantities, one could consider to modify the proposed model in order to minimize the desired 1P loadings simultaneously.

Figure 4 shows the residual pitch misalignment left on the rotor for $s^{(R)}$, as a function of the initial residual pitches $\epsilon^{(0)}$ and G grades. For more accurate results, only for these analyses the pitch actuator resolution was assumed to be 0.01 deg. Interestingly, the severity of the initial aerodynamic imbalance does not appear to play a role in the final rebalanced configuration. This is also consistent to what shown in [1], where the algorithm was mostly capable to rebalance the rotor irrespective of the initial aerodynamic imbalance. On the other hand, the inertial imbalance seems to affect the final pitch misalignment $\epsilon^{(R)}$, with a larger $\epsilon^{(R)}$ the larger the G grade. This can also be easily explained. The algorithm acts on the rotor by changing the pitch of the individual blades, with the aim of reducing a specific 1P fixed frame signal. In other words, the algorithm applies a specific aerodynamic imbalance to counteract the imbalance issues present on the rotor. If no mass imbalance is present, the algorithm will, ideally, generate an aerodynamic imbalance equal and opposite to the initial aerodynamic imbalance, meaning $\epsilon^{(R)} = 0$ deg. Let's now imagine that only a mass imbalance is present: the algorithm will introduce an aerodynamic imbalance to counteract the effect of the given mass imbalance, leading to a final $\epsilon^{(R)} \neq 0$ deg. Naturally, the larger the initial mass imbalance, the lager the aerodynamic imbalance introduced by the algorithm will be, thus perfectly explaining the results of Fig. 4.

Table 1. Wind inflow conditions over the algorithm iterations. TI: turbulence intensity; ϕ: yaw misalignment angle; κ: vertical shear.

Simulation	V [ms^{-1}]	TI [%]	ρ [kg/m^3]	ϕ [deg]	κ [-]
0	15	5	1.225	0	0.2
1	7	5	1.225	10	0.4
2	7	5	1.1	0	0.2
3	15	5	1.225	10	0.4
4	15	5	1.225	0	0.2

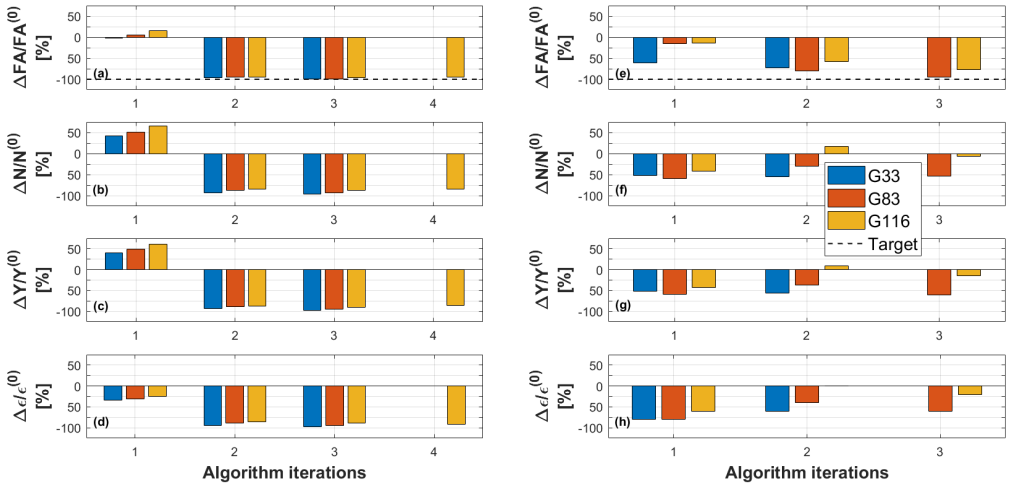

Figure 3. Variations of relevant parameters with respect to initial conditions as a function of algorithm iteration, for an initial aerodynamic imbalance $\epsilon^{(0)} = 3.5$ deg (left) and $\epsilon^{(0)} = 0.5$ deg (right). From top to bottom: variations in fore-aft acceleration; variation in nodding moment; variation in yawing moment; variation in ϵ.

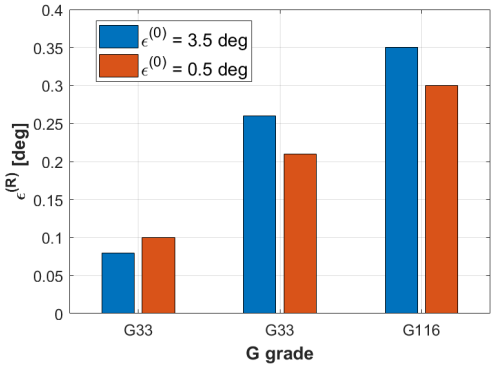

Figure 4. Residual pitch misalignment on the rotor after rebalancing $\epsilon^{(R)}$, as a function of different inertial imbalances and initial residual pitch misalignment $\epsilon^{(0)}$.

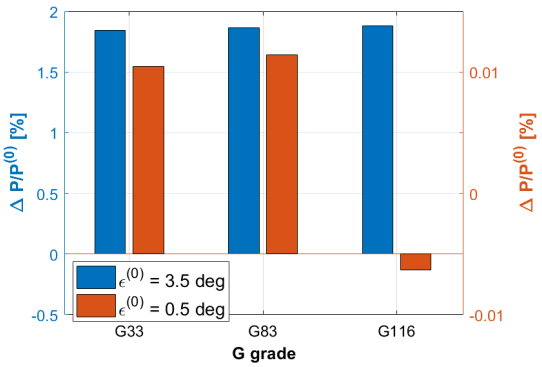

Figure 5. Power variations between rebalanced and imbalanced configurations at 7 m/s, as a function of different inertial imbalances and initial pitch misalignments: left y-axis (blue) for $\epsilon^{(0)} = 3.5$ deg; right y-axis (red) for $\epsilon^{(0)} = 0.5$ deg.

Still, the aerodynamic imbalance purposefully introduced by the algorithm might have consequences on the generated power, since the blade pitch angles might be different from the optimal ones. To quantify these effects, the rebalanced configurations $s^{(R)}$ found by the algorithm were simulated at 7 m/s, in region II. The generated power was then compared to the one achieved in the same ambient conditions by the respective imbalanced configuration $s^{(0)}$. Figure 5 shows that the aerodynamic imbalance generated by the algorithm does not negatively affect the produced power. On the contrary, the significantly reduced ϵ achieved for $\epsilon^{(0)} = 3.5$ deg allows for an increase in power production of about 1.8%. But small benefits can also be noted for $\epsilon^{(0)} = 0.5$ deg, whereas only for G116 a negligible power decrease of 0.002% in noted.

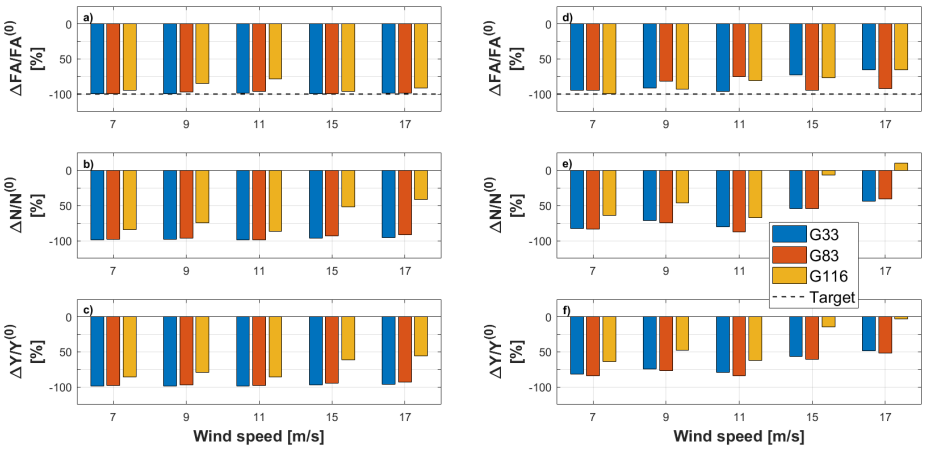

Figure 6. Performance of the rebalanced solutions with respect to the initial imbalanced configuration, as a function of wind speed, for an initial aerodynamic imbalance $\epsilon^{(0)} = 3.5$ deg (left) and $\epsilon^{(0)} = 0.5$ deg (right). From top to bottom: variations in fore-aft acceleration; variation in nodding moment; variation in yawing moment.

3.3. Dependency on operating point

As discussed in § 3.2, to rebalance the rotor the algorithm will introduce an aerodynamic imbalance to counteract the effects of the pre-existing imbalances. But given that aerodynamic and inertial imbalances depend on q and Ω^2 respectively, the rebalanced solution found by the algorithm might not be optimal for different operating conditions.

To mitigate this issue, the algorithm scales the 1P signals by the dynamic pressure. While this rescaling works well with aerodynamic imbalances, the same might not hold for mass imbalances. First of all, mass imbalances do not depend on density: a rescaling by q might lead to inaccuracies if density varies. Nevertheless, as proven in § 3.2, the iterative nature of the algorithm allows one to compensate for density changes. Secondly, the ratio $\frac{V}{\Omega R}$ is kept constant only in region II, making such rescaling less accurate outside the boundaries of this control region.

Therefore, to further characterize the algorithm performance, the rebalanced configurations $\mathrm{s}^{(\mathrm{R})}$ found in § 3.2 were tested at different wind speeds, while keeping the other relevant ambient parameters constant and equal to the ones of $\mathrm{s}^{(0)}$. This way, one can directly compare the 1P loading on the machine before and after rebalancing, for different operational points.

Figure 6 (left) shows the 1P variation between $\mathrm{s}^{(0)}$ and $\mathrm{s}^{(\mathrm{R})}$ for the larger initial aerodynamic imbalance $\epsilon^{(0)} = 3.5$ deg. The solution identified by the algorithm appears quite robust, being able to produce smaller 1P with respect to $\mathrm{s}^{(0)}$ seemingly independently on the wind speed. This holds for the fore-aft acceleration, again the parameter minimized, but also for other loads such as nodding and yawing moments.

Looking at the performance for $\epsilon^{(0)} = 0.5$ deg, Fig. 6 (right), similar conclusions can be drown. Nevertheless, a closer look at the results reveals how the yet good performance tends to degrade in region III, where the scaling correction is not exact. In addition, for a very large mass imbalance, although the fore-aft accelerations are still considerably reduced with respect to $\mathrm{s}^{(0)}$, the nodding moment slightly increases for higher wind speeds. Again, to deal with these issues one could adapt the algorithm to minimize more than one signal. Moreover, if the found solution were to strongly depend on the operating conditions, one could re-apply the algorithm to find a rebalanced configuration better suited for the given operating point.

4. Conclusions

In this paper, an already proposed rotor-rebalancing algorithm [1], which proved capable of remotely correcting for aerodynamic imbalances, was tested also on inertial imbalances. Several combinations of mass and aerodynamic imbalances were considered, introducing added masses and/or pitch offsets on one or more blades respectively. In addition, different turbulent inflows were also simulated, in order to best replicate realistic wind conditions. Based on the results here presented, the following conclusions can be drown.

- The method proved capable of significantly reducing the chosen 1P signal, i.e. rebalancing the rotor, also in the presence of a mass imbalance. Generally, only 3 to 4 iterations are required.
- Specifically, the algorithm purposefully introduced an aerodynamic imbalance - by applying a given pitch offset to each single blade - to compensate for the imbalances already present on the rotor.
- This newly introduced aerodynamic imbalances not only decrease vibrations in the fixed frame, but also do not seem to negatively affect the power production.
- The found rebalanced configurations seem quite robust with respect to changes not only in ambient conditions but also operating point, with a slight performance degradation in region III.

Although the algorithm aimed at reducing only the fore-aft main bearing accelerations, the performed tests showed how other relevant loads measured at the hub were also generally decreased, with minor exceptions. Nevertheless, given that inertial imbalances will generate different loading on different components depending on their lever arm, one might need to consider different drivers for the algorithm or combinations thereof, in order to minimize loading on the hub rather than on the tower, or on both. Additional studies in this sense might prove useful. Finally, the algorithm was still not validated in the field. Ad-hoc tests, where known initial imbalances are introduced on a real machine, would allow to evaluate the algorithm performance in real conditions.

References

[1] Bertelè M, Bottasso CL, and Cacciola S Automatic detection and correction of pitch misalignment in wind turbine rotors *Wind Energy Science* **2**:791–803 2018
[2] Blanco MI The economics of wind energy *Renewable and Sustainable Energy Reviews* **13**(6-7):1372–1382 2009
[3] Bottasso CL and Croce A Cp-lambda: user's manualuser's manual *Technical Report* Dipartimento di Ingegneria Aerospaziale, Politecnico di Milano 2006-16
[4] Cacciola C and Riboldi CED Equalizing aerodynamic blade loads through individual pitch control via multiblade multilag transformation *Journal of Solar Energy Engineering* **139**(6) 2017
[5] ISO ISO/1940-1:2003(E) August 2003
[6] Jonkman B and Kilcher L Turbsim users guide: version 1.06.00
[7] Kanev S and Engelen TG Exploring the limits in individual pitch control Proceedings of the European Wind Energy Conference Marseille France 2009
[8] Kusnick J, Adams DE and Griffith DT Wind turbine rotor imbalance detection using nacelle and blade measurements *Wind Energ* **18**(2):267–276 2015
[9] Niebsch J and Ramlau R Simultaneous estimation of mass and aerodynamic rotor imbalances for wind turbines *Journal of Mathematics in Industry* **4**(1):12 2014
[10] Niebsch J, Ramlau R and Nguyen TT Mass and aerodynamic imbalance estimates of wind turbines *Energies* **3**(4):696–710, 2010.
[11] Ramlau R and Niebsch J Imbalance estimation without test masses for wind turbines *J. Sol. Energy Eng* **13** 02 2009
[12] Riboldi CED Advanced control laws for variable-speed wind turbines and supporting enabling technologies
[13] Saathoff M, Rosemeier M, Kleinselbeck T and Rathmann B Effect of individual blade pitch angle misalignment on the remaining useful life of wind turbines Zenodo 2021.
[14] Wilkinson M, Hendriks B, Spinato F and Harman K Methodology and results of the Reliawind reliability field study European Wind Energy Conference Warsaw Poland 2010